

Multiple Topological Phase Transitions Unveiling Gapless Topological Superconductivity in Magnet/Unconventional Superconductor Hybrid Platform

Minakshi Subhadarshini,^{1,2, a)} Amartya Pal^{ib, 1,2, a)} Pritam Chatterjee^{ib, 1,2} and Arijit Saha^{ib 1,2, b)}

¹⁾ *Institute of Physics, Sachivalaya Marg, Bhubaneswar-751005, India,*

²⁾ *Homi Bhabha National Institute, Training School Complex, Anushakti Nagar, Mumbai 400094, India*

(Dated: 6 May 2024)

We propose a theoretical framework for generating gapless topological superconductivity (GTSC) hosting Majorana flat edge modes (MFEMs) in the presence of a two-dimensional (2D) array of magnetic adatoms with noncollinear spin texture deposited on top of a unconventional superconductor. Our observations reveal two distinct topological phase transitions within the emergent Shiba band depending on the exchange coupling strength (J) between magnetic adatom spins and superconducting electrons: the first one designates transition from gapless non-topological to gapless topological phase at lower J , while the second one denotes transition from gapless topological to a trivial gapped superconducting phase at higher J . The gapless topological superconducting phase survives at intermediate values of J , hosting MFEMs. Further, we investigate the nature of the bulk effective pairings which indicate that GTSC appears due to the interplay between pseudo “ s -wave” and pseudo “ $p_x + p_y$ ” types of pairing. Consequently, our study opens a promising avenue for the experimental realization of GTSC in 2D Shiba lattice based on d -wave superconductors as a high-temperature platform.

Topological superconductivity (TSC) hosting Majorana zero modes (MZMs) has emerged as one of the fascinating research areas in the modern quantum condensed matter physics community, due to its potential application in topological quantum computation and memory storage applications^{1–7}. There are several theoretical proposals that exist in the literature, which introduce the generation of isolated MZMs and their possible experimental feasibility^{1,4,8–12}. Few experimental setups have been fabricated based on these theoretical proposals, but they still pose significant challenges^{13–20}. In recent times, one of the most promising ways to generate TSC hosting MZMs relies on magnetic adatoms^{21–61}. According to this proposal, an array of magnetic adatoms with classical spins is fabricated on the surface of a bulk s -wave superconductor. This heterostructure can give rise to isolated MZMs at the end of the chain due to the scattering between the classical spin of magnetic adatoms and the spin of the superconducting electrons. Another interesting aspect of this setup is the formation of an emergent band within the superconducting gap in the presence of magnetic impurities. This is called the Yu-Shiba-Rusinov (YSR) band or simply the Shiba band^{21,22,62}. Experimentally, researchers have also observed the existence of the Shiba band^{51–61}, which plays the pivotal role during the topological phase transition. The sign change of the Shiba minigap indicates topological superconducting phase transition hosting MZMs^{21,22,53}.

In recent times, there has been a growing interest in the generation of MFEMs over MZMs for the memory storage

applications^{63–69}, which is a direct consequence of the 2D Kitaev model^{63,64}. In literature, the generation of MZMs involving Shiba states have been reported in several theoretical and experimental works based on unconventional superconductors^{70–75}. However, only a handful of recent articles have explored the engineering of MFEMs via magnet-superconductor heterostructures^{68,69}. Moreover, these proposals are based on conventional s -wave superconductors^{68,69}. Till date, no article is available in the literature, where the generation of MFEMs has been proposed resulting from the coexistence of magnet and unconventional superconductor hybrid system.

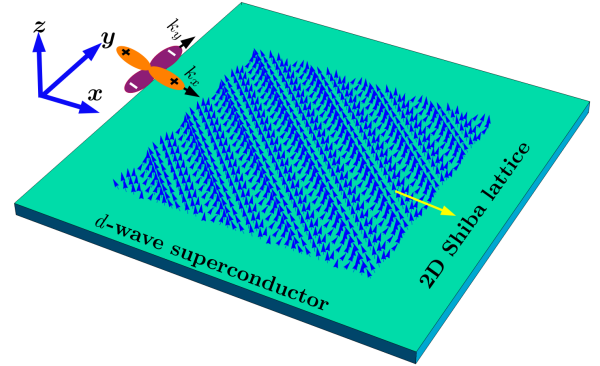


FIG. 1. Schematic diagram of our hybrid setup comprising of a 2D Shiba lattice with noncollinear magnetic texture (blue arrows), placed on top of a unconventional d -wave SC (green) with the d -wave nature of the pairing gap depicted in the x - y plane (top left).

^{a)}These authors contributed equally to this work.

^{b)}Electronic mail: arijit@iopb.res.in

In this article, we put forward a theoretical proposal for the emergence of the GTSC phase hosting MFEMs in the presence of a 2D array of noncollinear magnetic tex-

ture deposited on top of a d -wave superconductor (see Fig. 1 for a schematic view). Presence of exchange field inside a d -wave superconductor (SC) generates inflated topological Fermi surfaces^{76–79}. However, in this article, we primarily focus on the generation of MFEMs using noncollinear magnetism. Interestingly, we obtain two distinct topological phase transitions within the emergent 2D Shiba band, depending on the exchange coupling strength (J) between magnetic adatom spins and superconducting electrons: (i) the first one designates gapless non-topological to gapless topological phase transition at lower J , and (ii) the second one from gapless topological to a trivial gapped superconducting phase at higher J . The gapless topological phase resides at intermediate values of J , resulting in GTSC hosting MFEMs. Moreover, we compute the bulk effective pairings using a duality transformation of the low-energy continuum Hamiltonian. It suggests that the GTSC can be stabilized due to the interplay between pseudo “ s -wave” and pseudo “ $p_x + p_y$ ” types of pairings.

To begin with, we architect a toy model based on a 2D array of magnetic adatoms with noncollinear spin texture deposited on a unconventional d -wave superconductor as schematically shown in Fig. 1. The Bogoliubov de Gennes (BdG) Hamiltonian in the continuum limit can be written as, $\mathcal{H} = \int d\mathbf{r} \Psi^\dagger(\mathbf{r}) \mathcal{H}_{\text{BdG}} \Psi(\mathbf{r})$ where, $\Psi(\mathbf{r}) = [c_{\mathbf{r},\uparrow}, c_{\mathbf{r},\downarrow}, c_{\mathbf{r},\downarrow}^\dagger, -c_{\mathbf{r},\uparrow}^\dagger]^T$ is the Nambu spinor with $c_{r,\sigma}$ ($c_{r,\sigma}^\dagger$) being the electron annihilation (creation) operator with spin σ ($=\uparrow, \downarrow$) at position $\mathbf{r} = (x, y)$. The BdG Hamiltonian in the first quantized form can be written as,

$$\mathcal{H}_{\text{BdG}} = -\frac{\hbar^2}{2m} \nabla^2 \tau_z + JS(\mathbf{r}) \cdot \boldsymbol{\sigma} - \mu \tau_z + \Delta_d(\mathbf{r}) \tau_x, \quad (1)$$

Here, the Pauli matrices, τ and σ , act on particle hole and spin degrees of freedom respectively. J denotes the exchange coupling strength between magnetic impurities and superconducting electrons. Spin of the magnetic impurities is assumed to be classical and represented by an unit vector as $\mathbf{S}(\mathbf{r}) = (\sin \theta_r \cos \phi_r, \sin \theta_r \sin \phi_r, \cos \theta_r)$, where θ_r, ϕ_r being the polar and azimuthal angle at position \mathbf{r} . The symbols μ and $\Delta_d(\mathbf{r}) (= \Delta_0(\partial_x^2 - \partial_y^2))$ denotes the chemical potential and d -wave pairing amplitude of the superconductor respectively. For simplicity, we assume $\hbar = m = 1$ throughout the paper.

We perform two successive unitary transformations, $U_1 = e^{-i(\phi_r/2 - \pi/4)\sigma_z}$ and $U_2 = e^{-i(\theta_r/2 - \pi/4)\sigma_x}$ respectively, to obtain a translationally invariant low energy effective Hamiltonian as, $\mathcal{H}_{\text{eff}}(\mathbf{r}) = U_2^\dagger U_1^\dagger \mathcal{H}_{\text{BdG}}(\mathbf{r}) U_1 U_2$ ^{47,69,80}. Further, we choose, $\theta_r = (g_x x + g_y y)$ and $\phi_r = 0$ throughout the calculation. We also consider a homogeneous spin spiral (SS) by choosing $g_x = g_y = g$ for simplicity. The symbol g represents the pitch vector of the SS. The low energy effective Hamiltonian in the momentum-space can be written as,

$$\mathcal{H}_{\text{eff}}(\mathbf{k}) = \tilde{\xi}_{\mathbf{k}} \tau_z + \frac{g}{4} (k_x + k_y) \tau_z \sigma_x + \Delta_{\text{eff}} \tau_x + J \sigma_y, \quad (2)$$

where, $\tilde{\xi}_{\mathbf{k}} = \frac{1}{2}(\mathbf{k}^2 + \frac{g^2}{2}) - \mu$ and $\Delta_{\text{eff}} = \Delta_0[(k_x^2 - k_y^2) + \frac{g}{2}(k_x - k_y)\sigma_x]$. The term Δ_{eff} is comprised of the parent d -wave pairing amplitude and in addition, an emergent term ($p_x - p_y$) appears due to the presence of the 2D SS. The second term in Eq. (2) acts as an effective 2D spin orbit coupling (SOC) while the last term in Eq. (2) denotes an effective in plane Zeeman field along y -direction.

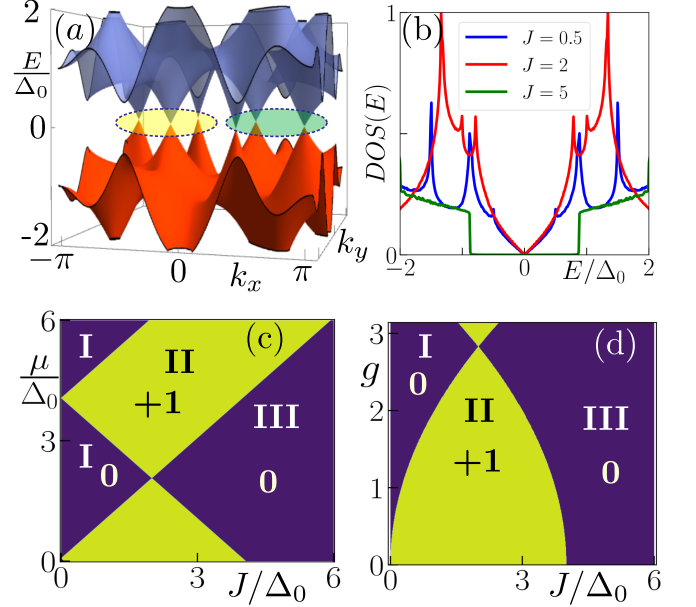


FIG. 2. Panel (a) displays the bulk band spectrum within the topological regime ($J = 2$), featuring six band touchings points. In panel (b), the bulk DOS is depicted for three phases: non-topological gapless ($J = 0.5$), topological gapless ($J = 2$), and gapped non-topological ($J = 5$). We choose $g = 2$ for panels(a)-(b). The invariant, ν , is demonstrated in the $\mu/\Delta_0 - J/\Delta_0$ plane choosing $g = 0.5$ in panel (c) and in the $g/\Delta_0 - J/\Delta_0$ plane in panel (d) with $\mu = 4$.

Furthermore, we compute the bulk topological invariant in order to characterize the gapless topological superconducting phase starting from the lattice regularized version of the Hamiltonian mentioned in Eq. (2). We replace $k_{x,y} \rightarrow \sin k_{x,y}$ and $k_{x,y}^2 \rightarrow 2(1 - \cos k_{x,y})$. The \mathcal{Z}_2 topological invariant denoted by ν , is defined as,^{68,69}

$$(-1)^\nu = \text{sgn} \prod_{i=1}^4 \det \begin{pmatrix} \xi_{\mathbf{k}}(\Gamma_i) - J & \Delta_d(\Gamma_i) \\ \Delta_d(\Gamma_i) & -\xi_{\mathbf{k}}(\Gamma_i) - J \end{pmatrix}, \quad (3)$$

where, $\nu = 0$ and $\nu = 1$ represent the topologically trivial and nontrivial regime respectively. The symbol $\Gamma = [(0, 0), (0, \pi), (\pi, 0), (\pi, \pi)]$ denotes the four high symmetry points of the square Brillouin zone. In Fig. 2(c) and Fig. 2(d), we illustrate the topological invariant in $\mu - J$ and $g - J$ plane respectively. Interestingly, we observe two topological phase transitions depending on the exchange coupling strength J for fixed values of μ and g . We obtain two types of topologically trivial phases with $\nu = 0$ (labelled as I and III in Fig. 2) separated by a

topologically non-trivial phase with $\nu = 1$ (indicated as II in Fig. 2). To further investigate these different phases, we compute the bulk density of states (DOS), $\text{DOS}(E) = (1/\pi) \sum_{\mathbf{k}} \delta(E - E_{\mathbf{k}})$ which is depicted in Fig. 2(b) for three distinct values of J , representing three phases I, II and III. The latter is denoted by blue, red and green color line respectively. Thus, the system undergoes two phase transitions from (i) gapless non-topological to gapless topological phase and (ii) gapless topological to gapped non-topological phase within the emergent Shiba band [see Figs. 2(c)-(d)]. We identify the GTSC with six band touching points associated with semimetallic DOS in the topological regime (phase II) from bulk band structure and DOS as shown in Figs. 2(a)-(b). On the other hand, two non-topological phases exhibit both gapped and semimetallic DOS tunable by exchange coupling strength J [see Fig. 2((b))].

To examine the nature of bulk effective pairing we perform a unitary transformation,^{47,81,82} in order to obtain a dual Hamiltonian of Eq. (2), $\tilde{\mathcal{H}}_D = \tilde{U}^\dagger \mathcal{H}_{\text{eff}} \tilde{U}$ as,

$$\tilde{U} = \frac{1}{\sqrt{2}} \begin{pmatrix} 1 & -1 \\ 1 & 1 \end{pmatrix} \sigma_0; \tilde{\mathcal{H}}_D = \begin{pmatrix} \tilde{\xi}_{\mathbf{k}}^D \sigma_z + J \sigma_y & \tilde{\Delta}_D \\ \tilde{\Delta}_D & -\tilde{\xi}_{\mathbf{k}}^D \sigma_z + J \sigma_y \end{pmatrix}, \quad (4)$$

where, $\tilde{\xi}_{\mathbf{k}}^D = \frac{g}{2}(k_x - k_y)$ and $\tilde{\Delta}_D = \tilde{\Delta}_s \sigma_0 + \tilde{\Delta}_p \sigma_x = (2 - \mu + g^2/4)\sigma_0 + (g/4)(k_x + k_y)\sigma_x$ are called dual kinetic energy and dual SC like gap of the transformed Hamiltonian. Here we neglect $O(k^2)$ terms at the low energy limit. The dual spinor takes the form in pseudo Nambu basis as, $\tilde{\Psi}(\mathbf{k}) = [\tilde{c}_{\mathbf{k},+}, \tilde{c}_{\mathbf{k},-}, \tilde{c}_{\mathbf{k},-}^\dagger, -\tilde{c}_{\mathbf{k},+}^\dagger]^T$, where, $\tilde{c}_{\mathbf{k},+(-)} = (c_{\mathbf{k},\uparrow(\downarrow)} + (-)c_{-\mathbf{k},\downarrow(\uparrow)}^\dagger)/\sqrt{2}$ mimics a system with pseudo-spin degree of freedom. Therefore, the effective pairing/dual gap ($\tilde{\Delta}_D$) turns out to be the combination of a pseudo s -wave ($\tilde{\Delta}_s$) and a pseudo ($p_x + p_y$) ($\tilde{\Delta}_p$) type pairings in the topological phase (II). Hence, the emergence of the pseudo ($p_x + p_y$) type pairing is the direct consequence of the nonlinear magnetic texture that stabilizes the gapless topological phase II hosting MFEMs^{63,64,67-69} which we discuss in detail in the latter text.

To investigate the boundary of our 2D system, we analyze our results based on finite geometry calculations performed via the lattice-regularized version of the Hamiltonian in Eq. (2). In Figs. 3(a)-(c), we illustrate the eigenvalue spectrum as a function of momentum k_y , considering open boundary conditions (OBC) along the x direction and periodic boundary conditions (PBC) along the y direction. Therefore, momentum along the y direction (k_y) is a good quantum number. Here, Fig. 3(a), Fig. 3(b), and Fig. 3(c) correspond to the three phases I, II, and III, respectively, as depicted in Fig. 2. Interestingly, the topological phase (phase II) unveils the emergence of three gapless MFEMs between bulk band touching points [see Fig. 3(b)]. This is a consequence of six gapless nodes in the bulk [see Fig. 2(a)]. Hence, qualitatively, we can predict that the GTSC anchoring MFEMs can be stabilized due to the presence of pseudo

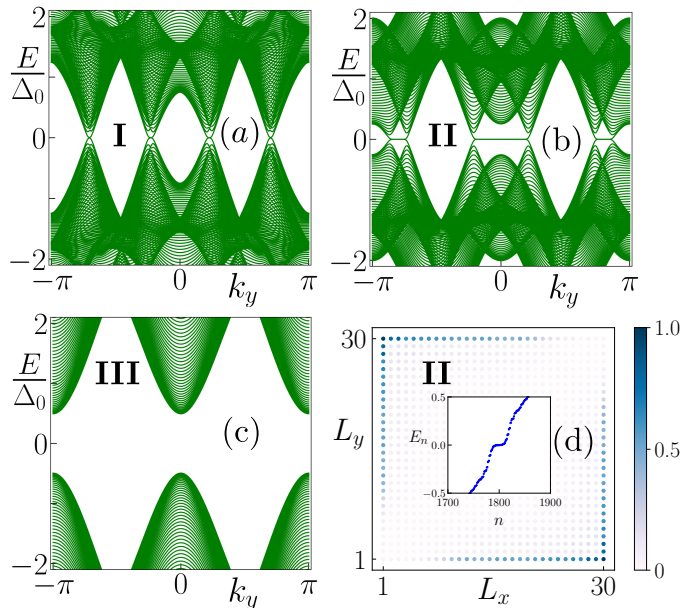


FIG. 3. Panels (a)-(c) depict the energy eigenvalue spectrum considering the ribbon geometry, revealing the presence of multiple zero-energy flat edge modes in the topological regime [(b) $J = 2$]. This stands in sharp contrast to the absence of such modes in the trivial region [(a) $J = 0.5$, and (c) $J = 5$]. Panel (d) displays the normalized site resolved LDOS at $E = 0$ corresponding to the MEFM, computed within a 30×30 square lattice. In all cases, we choose the model parameters as $\Delta_0 = 1$, $t = 1$, $g = 3$ and $\mu = 4$.

“ s -wave” and pseudo “ $p_x + p_y$ ” type pairing (as discussed before). On the other hand, in the non-topological phases (phase I and III in Fig. 2), the system is either gapless or gapped without hosting any types of edge mode as shown in Figs. 3(a) and (c). In Fig. 3(d), we compute the normalized local density of states (LDOS) at $E = 0$ in the $L_x - L_y$ plane associated with phase II. We consider OBC along both the x and y directions, employing the formula $N_i(E) = \sum_n |\phi_n(i)|^2 \delta(E - E_n)$, where $\phi_n(i)$ is the eigenstate of the Hamiltonian at site i . The symbol n is the eigenvalue index with eigenvalue E_n . It is evident from the LDOS distribution that zero-energy eigenstates are maximally localized at the edges (MFEMs), which is also reflected in the E_n vs n behavior via the inset of the same figure. Note that, the location of the edge modes are not constrained to be appeared at the negative diagonal of the 2D domain. Edge states can also appear in the positive diagonal of the system by changing the spin texture configuration from $\theta_r = (g_x x + g_y y)$ to $\theta_r = (g_x x - g_y y)$ in the effective Hamiltonian. This observation confirms that our model harbors Majorana flat modes localized at the edges, thereby establishing the bulk-boundary correspondence of the system.

Furthermore, we compute the spectral function, $\mathcal{A}(k_x, \omega) = -\frac{1}{\pi} \text{Im}[\text{Tr} \mathcal{G}(k_x, \omega)]$ with $\mathcal{G}(k_x, \omega) = [(\omega + i\epsilon)\mathcal{I} - \mathcal{H}(y, k_x)]^{-1}$ using the lattice regularized Hamiltonian of Eq. (2) and employing OBC along y direction and PBC

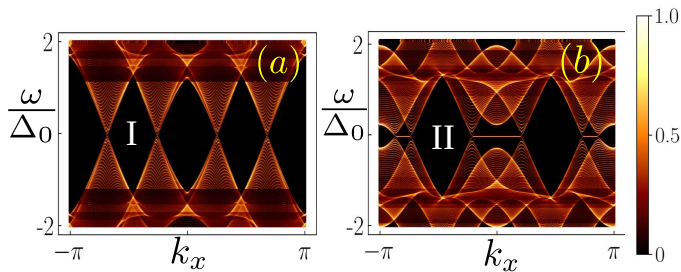


FIG. 4. Spectral function, $\mathcal{A}(k, \omega)$ is shown in $(\omega/\Delta_0 - k_x)$ plane for (a) gapless non-topological phase ($J = 0.5$), (b) gapless topological phase ($J = 2$). We choose the model parameters as $\Delta_0 = 1$, $t = 1$, $g = 3$ and $\mu = 4$.

along x direction. In Fig. 4, we depict the behavior of $\mathcal{A}(k, \omega)$ in $(\omega/\Delta_0 - k_x)$ plane. Here, we discuss the two phases: (i) the gapless non-topological phase and (ii) the gapless topological phase. We observe a clear signature of MFEMs in the topological regime [see Fig. 4(b)]. On the other hand, MFEMs disappear in the gapless non-topological regime as shown in Fig. 4(a). From practical point of view, it can be possible to measure $\mathcal{A}(k_x, \omega)$ in terms of angle-resolved photoemission spectroscopy (ARPES) to look for the signature of MFEMs.

In this article, we systematically investigate the emergence of GTSC phase hosting MFEMs in the presence of a 2D array of a magnetic adatoms characterized by a spatially modulated noncollinear spin texture implemented on an unconventional superconductor (with d -wave pairing symmetry) as a high-temperature platform. To elucidate further on the system's topological properties, we derive the low-energy effective Hamiltonian in k -space through two successive unitary transformations. Furthermore, we compute the \mathcal{Z}_2 topological invariant and bulk DOS to characterize the bulk of the system. Importantly, we find three distinct scenarios: (i) a gapless non-topological phase, (ii) a gapless topological phase hosting multiple MFEMs, and (iii) a gapped non-topological phase (as shown in Fig. 2). Finally, we unveil the appearance of multiple MFEMs, maximally localized at the system edges in the topological regime, through ribbon geometry and finite-size lattice simulations. We further compute the spectral function numerically which clearly suggests the appearance of the MFEMs at the boundary of the system. However, note that experimentally detecting the MFEMs via $\mathcal{A}(k, \omega)$ can be extremely challenging as bulk states can penetrate substantially due to the gapless nature. One possible way to realize a gapped spectrum for our case is to deposit a layer of 2D quantum spin Hall insulator on top of the composite system (d -wave superconductor + non-collinear spin texture), following the same route as demonstrated in⁴⁷. However, the nature of the bulk topology of such composite system is expected to be different, leading to a second-order topological superconductor, which is beyond the scope of the present manuscript and will be presented elsewhere.

The possible experimental realization of our setup in-

volves the placement of a monolayer of magnetic adatoms (such as Fe/Cr/Mn) deposited on top of an iron-based superconducting substrate (such as FeSe, β -Fe1.01Se, LaFeAs, etc.). Such configuration has attracted significant recent attention in the context of experimental realization of topological superconductivity, hosting MZMs in high-temperature platforms^{75,83–87}. Notably, the emergence of in-gap Shiba states, in addition to Majorana bound states, has been observed in FeTe0.55Se0.45 superconductors^{75,86}. Therefore, given the experimental progress in this research field, we believe that our theoretical model proposal for GTSC hosting MFEMs is timely and may be possible to realize in future experiments. However, the exact description of experimental techniques and prediction of candidate materials based on our model Hamiltonian are not the subject matter of our present manuscript.

ACKNOWLEDGMENTS

A.P. acknowledge the SAMKHYA: HPC Facility provided at IOP, Bhubaneswar, for numerical computations. We acknowledge Department of Atomic Energy (DAE), Govt. of India for providing the financial support.

- ¹A. Y. Kitaev, "Unpaired majorana fermions in quantum wires," *Physics-Uspekhi* **44**, 131 (2001).
- ²D. A. Ivanov, "Non-abelian statistics of half-quantum vortices in p -wave superconductors," *Phys. Rev. Lett.* **86**, 268–271 (2001).
- ³C. Nayak, S. H. Simon, A. Stern, M. Freedman, and S. Das Sarma, "Non-abelian anyons and topological quantum computation," *Rev. Mod. Phys.* **80**, 1083–1159 (2008).
- ⁴A. Kitaev, "Periodic table for topological insulators and superconductors," *AIP Conference Proceedings* **1134**, 22–30 (2009).
- ⁵J. Alicea, "New directions in the pursuit of majorana fermions in solid state systems," *Reports on Progress in Physics* **75**, 076501 (2012).
- ⁶M. Leijnse and K. Flensberg, "Introduction to topological superconductivity and majorana fermions," **27**, 124003 (2012).
- ⁷C. Beenakker, "Search for majorana fermions in superconductors," *Annual Review of Condensed Matter Physics* **4**, 113–136 (2013).
- ⁸N. Read and D. Green, "Paired states of fermions in two dimensions with breaking of parity and time-reversal symmetries and the fractional quantum hall effect," *Phys. Rev. B* **61**, 10267–10297 (2000).
- ⁹L. Fu and C. L. Kane, "Superconducting proximity effect and majorana fermions at the surface of a topological insulator," *Phys. Rev. Lett.* **100**, 096407 (2008).
- ¹⁰Y. Oreg, G. Refael, and F. von Oppen, "Helical liquids and majorana bound states in quantum wires," *Phys. Rev. Lett.* **105**, 177002 (2010).
- ¹¹R. M. Lutchyn, J. D. Sau, and S. Das Sarma, "Majorana fermions and a topological phase transition in semiconductor-superconductor heterostructures," *Phys. Rev. Lett.* **105**, 077001 (2010).
- ¹²S. Kanasugi and Y. Yanase, "Multiorbital ferroelectric superconductivity in doped strontium," *Phys. Rev. B* **100**, 094504 (2019).
- ¹³V. Mourik, K. Zuo, S. M. Frolov, S. R. Plissard, E. P. A. M. Bakkers, and L. P. Kouwenhoven, "Signatures of majorana fermions in hybrid superconductor-semiconductor nanowire devices," *Science* **336**, 1003–1007 (2012).
- ¹⁴A. Das, Y. Ronen, Y. Most, Y. Oreg, M. Heiblum, and H. Shtrikman, "Zero-bias peaks and splitting in an al-inas nanowire topo-

- logical superconductor as a signature of majorana fermions,” *Nature Physics* **8**, 887–895 (2012).
- ¹⁵L. P. Rokhinson, X. Liu, and J. K. Furdyna, “The fractional a.c. josephson effect in a semiconductor–superconductor nanowire as a signature of majorana particles,” *Nature Physics* **8**, 795–799 (2012).
- ¹⁶A. D. K. Finck, D. J. Van Harlingen, P. K. Mohseni, K. Jung, and X. Li, “Anomalous modulation of a zero-bias peak in a hybrid nanowire-superconductor device,” *Phys. Rev. Lett.* **110**, 126406 (2013).
- ¹⁷S. M. Albrecht, A. P. Higginbotham, M. Madsen, F. Kuemmeth, T. S. Jespersen, J. Nygård, P. Krogstrup, and C. M. Marcus, “Exponential protection of zero modes in majorana islands,” *Nature* **531**, 206–209 (2016).
- ¹⁸M. T. Deng, S. Vaitiekėnas, E. B. Hansen, J. Danon, M. Leijnse, K. Flensberg, J. Nygård, P. Krogstrup, and C. M. Marcus, “Majorana bound state in a coupled quantum-dot hybrid-nanowire system,” *Science* **354**, 1557–1562 (2016).
- ¹⁹T. Schumann, L. Galletti, H. Jeong, K. Ahadi, W. M. Strickland, S. Salmani-Rezaie, and S. Stemmer, “Possible signatures of mixed-parity superconductivity in doped polar SrTiO₃ films,” *Phys. Rev. B* **101**, 100503 (2020).
- ²⁰K. Ahadi, L. Galletti, Y. Li, S. Salmani-Rezaie, W. Wu, and S. Stemmer, “Enhancing superconductivity in srtio₃sub_z3i/sub_z films with strain,” *Science Advances* **5**, eaaw0120 (2019).
- ²¹F. Pientka, L. I. Glazman, and F. von Oppen, “Topological superconducting phase in helical shiba chains,” *Phys. Rev. B* **88**, 155420 (2013).
- ²²S. Nadj-Perge, I. K. Drozdov, B. A. Bernevig, and A. Yazdani, “Proposal for realizing majorana fermions in chains of magnetic atoms on a superconductor,” *Phys. Rev. B* **88**, 020407 (2013).
- ²³J. Klinovaja, P. Stano, A. Yazdani, and D. Loss, “Topological superconductivity and majorana fermions in rkky systems,” *Phys. Rev. Lett.* **111**, 186805 (2013).
- ²⁴B. Braunecker and P. Simon, “Interplay between classical magnetic moments and superconductivity in quantum one-dimensional conductors: Toward a self-sustained topological majorana phase,” *Phys. Rev. Lett.* **111**, 147202 (2013).
- ²⁵M. M. Vazifeh and M. Franz, “Self-organized topological state with majorana fermions,” *Phys. Rev. Lett.* **111**, 206802 (2013).
- ²⁶J. D. Sau and E. Demler, “Bound states at impurities as a probe of topological superconductivity in nanowires,” *Phys. Rev. B* **88**, 205402 (2013).
- ²⁷F. Pientka, L. I. Glazman, and F. von Oppen, “Unconventional topological phase transitions in helical shiba chains,” *Phys. Rev. B* **89**, 180505 (2014).
- ²⁸K. Pöyhönen, A. Westström, J. Röntynen, and T. Ojanen, “Majorana states in helical shiba chains and ladders,” *Phys. Rev. B* **89**, 115109 (2014).
- ²⁹I. Reis, D. J. J. Marchand, and M. Franz, “Self-organized topological state in a magnetic chain on the surface of a superconductor,” *Phys. Rev. B* **90**, 085124 (2014).
- ³⁰W. Hu, R. T. Scalettar, and R. R. P. Singh, “Interplay of magnetic order, pairing, and phase separation in a one-dimensional spin-fermion model,” *Phys. Rev. B* **92**, 115133 (2015).
- ³¹H.-Y. Hui, P. M. R. Brydon, J. D. Sau, S. Tewari, and S. D. Sarma, “Majorana fermions in ferromagnetic chains on the surface of bulk spin-orbit coupled s-wave superconductors,” *Scientific Reports* **5**, 8880 (2015).
- ³²S. Hoffman, J. Klinovaja, and D. Loss, “Topological phases of inhomogeneous superconductivity,” *Phys. Rev. B* **93**, 165418 (2016).
- ³³M. H. Christensen, M. Schechter, K. Flensberg, B. M. Andersen, and J. Paaske, “Spiral magnetic order and topological superconductivity in a chain of magnetic adatoms on a two-dimensional superconductor,” *Phys. Rev. B* **94**, 144509 (2016).
- ³⁴G. Sharma and S. Tewari, “Yu-shiba-rusinov states and topological superconductivity in ising paired superconductors,” *Phys. Rev. B* **94**, 094515 (2016).
- ³⁵G. M. Andolina and P. Simon, “Topological properties of chains of magnetic impurities on a superconducting substrate: Interplay between the shiba band and ferromagnetic wire limits,” *Phys. Rev. B* **96**, 235411 (2017).
- ³⁶V. Kaladzhyan, P. Simon, and M. Trif, “Controlling topological superconductivity by magnetization dynamics,” *Phys. Rev. B* **96**, 020507 (2017).
- ³⁷A. Theiler, K. Björnson, and A. M. Black-Schaffer, “Majorana bound state localization and energy oscillations for magnetic impurity chains on conventional superconductors,” *Phys. Rev. B* **100**, 214504 (2019).
- ³⁸D. Sticlet and C. Morari, “Topological superconductivity from magnetic impurities on monolayer nbse₂,” *Phys. Rev. B* **100**, 075420 (2019).
- ³⁹M. Mashkooori and A. Black-Schaffer, “Majorana bound states in magnetic impurity chains: Effects of *d*-wave pairing,” *Phys. Rev. B* **99**, 024505 (2019).
- ⁴⁰G. C. Ménard, C. Brun, R. Leriche, M. Trif, F. Debontridder, D. Demaille, D. Roditchev, P. Simon, and T. Cren, “Yu-shiba-rusinov bound states versus topological edge states in Pb/Si(111),” *The European Physical Journal Special Topics* **227**, 2303–2313 (2019).
- ⁴¹M. Mashkooori, S. Pradhan, K. Björnson, J. Fransson, and A. M. Black-Schaffer, “Identification of topological superconductivity in magnetic impurity systems using bulk spin polarization,” *Phys. Rev. B* **102**, 104501 (2020).
- ⁴²R. L. R. C. Teixeira, D. Kuzmanovski, A. M. Black-Schaffer, and L. G. G. V. D. da Silva, “Enhanced majorana bound states in magnetic chains on superconducting topological insulator edges,” *Phys. Rev. B* **102**, 165312 (2020).
- ⁴³S. Rex, I. V. Gornyi, and A. D. Mirlin, “Majorana modes in emergent-wire phases of helical and cycloidal magnet-superconductor hybrids,” *Phys. Rev. B* **102**, 224501 (2020).
- ⁴⁴V. Perrin, M. Civelli, and P. Simon, “Identifying majorana bound states by tunneling shot-noise tomography,” *Phys. Rev. B* **104**, L121406 (2021).
- ⁴⁵A. Kobińska, N. Sedlmayr, M. M. Maška, and T. Domański, “Dimerization-induced topological superconductivity in a rashba nanowire,” *Phys. Rev. B* **101**, 085402 (2020).
- ⁴⁶P. Chatterjee, S. Pradhan, A. K. Nandy, and A. Saha, “Tailoring the phase transition from topological superconductor to trivial superconductor induced by magnetic textures of a spin chain on a *p*-wave superconductor,” *Phys. Rev. B* **107**, 085423 (2023).
- ⁴⁷P. Chatterjee, A. K. Ghosh, A. K. Nandy, and A. Saha, “Second-order topological superconductor via noncollinear magnetic texture,” (2023), [arXiv:2308.12703 \[cond-mat.mes-hall\]](https://arxiv.org/abs/2308.12703).
- ⁴⁸D. Mondal, A. K. Ghosh, T. Nag, and A. Saha, “Engineering anomalous floquet majorana modes and their time evolution in a helical shiba chain,” *Phys. Rev. B* **108**, L081403 (2023).
- ⁴⁹G. Yang, P. Stano, J. Klinovaja, and D. Loss, “Majorana bound states in magnetic skyrmions,” *Phys. Rev. B* **93**, 224505 (2016).
- ⁵⁰K. Pöyhönen, A. Westström, S. S. Pershoguba, T. Ojanen, and A. V. Balatsky, “Skyrmion-induced bound states in a *p*-wave superconductor,” *Phys. Rev. B* **94**, 214509 (2016).
- ⁵¹A. Yazdani, B. A. Jones, C. P. Lutz, M. F. Crommie, and D. M. Eigler, “Probing the local effects of magnetic impurities on superconductivity,” *Science* **275**, 1767–1770 (1997).
- ⁵²A. Yazdani, C. M. Howald, C. P. Lutz, A. Kapitulnik, and D. M. Eigler, “Impurity-induced bound excitations on the surface of Bi₂Sr₂CaCu₂O₈,” *Phys. Rev. Lett.* **83**, 176–179 (1999).
- ⁵³A. Yazdani, “Visualizing majorana fermions in a chain of magnetic atoms on a superconductor,” *Physica Scripta* **2015**, 014012 (2015).
- ⁵⁴L. Schneider, P. Beck, T. Posske, D. Crawford, E. Mascot, S. Rachel, R. Wiesendanger, and J. Wiebe, “Topological shiba bands in artificial spin chains on superconductors,” *Nature Physics* **17**, 943–948 (2021).
- ⁵⁵P. Beck, L. Schneider, L. Rózsa, K. Palotás, A. Lászlóffy, L. Szunyogh, J. Wiebe, and R. Wiesendanger, “Spin-orbit coupling induced splitting of Yu-Shiba-Rusinov states in antiferromagnetic dimers,” *Nature Communications* **12**, 2040 (2021).

- ⁵⁶D. Wang, J. Wiebe, R. Zhong, G. Gu, and R. Wiesendanger, “Spin-polarized yu-shiba-rusinov states in an iron-based superconductor,” *Phys. Rev. Lett.* **126**, 076802 (2021).
- ⁵⁷L. Schneider, P. Beck, J. Neuhaus-Steinmetz, L. Rózsa, T. Posske, J. Wiebe, and R. Wiesendanger, “Precursors of majorana modes and their length-dependent energy oscillations probed at both ends of atomic shiba chains,” *Nature Nanotechnology* **17**, 384–389 (2022).
- ⁵⁸F. Küster, S. Brinker, R. Hess, D. Loss, S. S. P. Parkin, J. Klinovaja, S. Lounis, and P. Sessi, “Non-majorana modes in diluted spin chains proximitized to a superconductor,” *Proceedings of the National Academy of Sciences* **119**, e2210589119 (2022).
- ⁵⁹R. Lo Conte, M. Bazarnik, K. Palotás, L. Rózsa, L. Szunyogh, A. Kubetzka, K. von Bergmann, and R. Wiesendanger, “Coexistence of antiferromagnetism and superconductivity in Mn/Nb(110),” *Phys. Rev. B* **105**, L100406 (2022).
- ⁶⁰A. Yazdani, F. von Oppen, B. I. Halperin, and A. Yacoby, “Hunting for majoranas,” *Science* **380**, eade0850 (2023).
- ⁶¹M. O. Soldini, F. Küster, G. Wagner, S. Das, A. Aldarawsheh, R. Thomale, S. Lounis, S. S. P. Parkin, P. Sessi, and T. Neupert, “Two-dimensional shiba lattices as a possible platform for crystalline topological superconductivity,” *Nature Physics* (2023), 10.1038/s41567-023-02104-5.
- ⁶²H. Shiba, “Classical Spins in Superconductors,” *Progress of Theoretical Physics* **40**, 435–451 (1968).
- ⁶³P. Wang, S. Lin, G. Zhang, and Z. Song, “Topological gapless phase in kitaev model on square lattice,” *Scientific Reports* **7**, 17179 (2017).
- ⁶⁴K. L. Zhang, P. Wang, and Z. Song, “Majorana flat band edge modes of topological gapless phase in 2d kitaev square lattice,” *Scientific Reports* **9**, 4978 (2019).
- ⁶⁵C. L. M. Wong, J. Liu, K. T. Law, and P. A. Lee, “Majorana flat bands and unidirectional majorana edge states in gapless topological superconductors,” *Phys. Rev. B* **88**, 060504 (2013).
- ⁶⁶S. Deng, G. Ortiz, A. Poudel, and L. Viola, “Majorana flat bands in s -wave gapless topological superconductors,” *Phys. Rev. B* **89**, 140507 (2014).
- ⁶⁷S. Nakosai, Y. Tanaka, and N. Nagaosa, “Two-dimensional p -wave superconducting states with magnetic moments on a conventional s -wave superconductor,” *Phys. Rev. B* **88**, 180503 (2013).
- ⁶⁸N. Sedlmayr, J. M. Aguiar-Hualde, and C. Bena, “Flat majorana bands in two-dimensional lattices with inhomogeneous magnetic fields: Topology and stability,” *Phys. Rev. B* **91**, 115415 (2015).
- ⁶⁹P. Chatterjee, S. Banik, S. Bera, A. K. Ghosh, S. Pradhan, A. Saha, and A. K. Nandy, “Topological superconductivity by engineering noncollinear magnetism in magnet/ superconductor heterostructures: A realistic prescription for 2d kitaev model,” (2023), arXiv:2303.03938 [cond-mat.mes-hall].
- ⁷⁰F. Pientka, L. I. Glazman, and F. von Oppen, “Unconventional topological phase transitions in helical shiba chains,” *Phys. Rev. B* **89**, 180505 (2014).
- ⁷¹A. Kreisel, T. Hyart, and B. Rosenow, “Tunable topological states hosted by unconventional superconductors with adatoms,” *Phys. Rev. Res.* **3**, 033049 (2021).
- ⁷²T. Neupert, A. Yazdani, and B. A. Bernevig, “Shiba chains of scalar impurities on unconventional superconductors,” *Phys. Rev. B* **93**, 094508 (2016).
- ⁷³D. Crawford, E. Mascot, D. K. Morr, and S. Rachel, “High-temperature majorana fermions in magnet-superconductor hybrid systems,” *Phys. Rev. B* **101**, 174510 (2020).
- ⁷⁴A. Ghazaryan, A. Kirmani, R. M. Fernandes, and P. Ghaemi, “Anomalous shiba states in topological iron-based superconductors,” *Phys. Rev. B* **106**, L201107 (2022).
- ⁷⁵D. Chatzopoulos, D. Cho, K. M. Bastiaans, G. O. Steffensen, D. Bouwmeester, A. Akbari, G. Gu, J. Paaske, B. M. Andersen, and M. P. Allan, “Spatially dispersing yu-shiba-rusinov states in the unconventional superconductor fete0.55se0.45,” *Nature Communications* **12**, 298 (2021).
- ⁷⁶K. Yang and S. L. Sondhi, “Response of a $d_{x^2-y^2}$ superconductor to a zeeman magnetic field,” *Phys. Rev. B* **57**, 8566–8570 (1998).
- ⁷⁷C. Setty, Y. Cao, A. Kreisel, S. Bhattacharyya, and P. J. Hirschfeld, “Bogoliubov fermi surfaces in spin- $\frac{1}{2}$ systems: Model hamiltonians and experimental consequences,” *Phys. Rev. B* **102**, 064504 (2020).
- ⁷⁸C. Setty, S. Bhattacharyya, Y. Cao, A. Kreisel, and P. J. Hirschfeld, “Topological ultranodal pair states in iron-based superconductors,” *Nature Communications* **11**, 523 (2020).
- ⁷⁹A. Pal, A. Saha, and P. Dutta, “Transport signatures of bogoliubov fermi surfaces in normal metal/time-reversal symmetry broken d -wave superconductor junctions,” (2023), arXiv:2308.07376 [cond-mat.supr-con].
- ⁸⁰R. Hess, H. F. Legg, D. Loss, and J. Klinovaja, “Josephson transistor from the superconducting diode effect in domain wall and skyrmion magnetic racetracks,” *Phys. Rev. B* **108**, 174516 (2023).
- ⁸¹M. Sato, Y. Takahashi, and S. Fujimoto, “Non-abelian topological order in s -wave superfluids of ultracold fermionic atoms,” *Phys. Rev. Lett.* **103**, 020401 (2009).
- ⁸²M. Sato, Y. Takahashi, and S. Fujimoto, “Non-abelian topological orders and majorana fermions in spin-singlet superconductors,” *Phys. Rev. B* **82**, 134521 (2010).
- ⁸³D. Wang, L. Kong, P. Fan, H. Chen, S. Zhu, W. Liu, L. Cao, Y. Sun, S. Du, J. Schneeloch, R. Zhong, G. Gu, L. Fu, H. Ding, and H.-J. Gao, “Evidence for majorana bound states in an iron-based superconductor,” *Science* **362**, 333–335 (2018).
- ⁸⁴F.-C. Hsu, J.-Y. Luo, K.-W. Yeh, T.-K. Chen, T.-W. Huang, P. M. Wu, Y.-C. Lee, Y.-L. Huang, Y.-Y. Chu, D.-C. Yan, and M.-K. Wu, “Superconductivity in the pbo-type structure α fese,” *Proceedings of the National Academy of Sciences* **105**, 14262–14264 (2008).
- ⁸⁵S. Medvedev, T. M. McQueen, I. A. Troyan, T. Palasyuk, M. I. Erements, R. J. Cava, S. Naghavi, F. Casper, V. Ksenofontov, G. Wortmann, and C. Felser, “Electronic and magnetic phase diagram of β -fe1.01se with superconductivity at 36.7 k under pressure,” *Nature Materials* **8**, 630–633 (2009).
- ⁸⁶P. Zhang, K. Yaji, T. Hashimoto, Y. Ota, T. Kondo, K. Okazaki, Z. Wang, J. Wen, G. D. Gu, H. Ding, and S. Shin, “Observation of topological superconductivity on the surface of an iron-based superconductor,” *Science* **360**, 182–186 (2018).
- ⁸⁷Y. Kamihara, T. Watanabe, M. Hirano, and H. Hosono, “Iron-based layered superconductor $\text{La}[\text{o}1\text{-xfx}]\text{Feas}$ ($x = 0.05\text{-}0.12$) with $t_c = 26$ k,” *Journal of the American Chemical Society* **130**, 3296–3297 (2008).